CHEMISTRY OF MATERIALS

pubs.acs.org/cm

Comments

Particle Size Is a Primary Determinant for Sigmoidal Kinetics of Nanoparticle Formation: A "Disproof" of the Finke–Watzky (F-W) Nanoparticle Nucleation and Growth Mechanism

Cite This: *Chem. Mater.* 2020, 32, 3651–3656

Read Online

ACCESS | Metrics & More | Article Recommendations | Supporting Information

Understanding the mechanism(s) by which nanoparticles are formed is a challenging problem but one that can provide valuable insight with respect to advanced materials design. Models to describe such nanoparticle formation remain somewhat controversial. In 1997, Finke and Watzky proposed,[1] and subsequently have published extensively (e.g., refs 2–8), a mechanistic model for nanoparticle formation kinetics that is based on the conception of continuous nucleation followed by autocatalytic surface growth. This F-W model describes microsteps,

$$A \xrightarrow{k_1} B \qquad \text{(nucleation)}$$

$$A + B \xrightarrow{k_2} 2B \qquad \text{(autocatalytic surface growth)}$$

Solving the corresponding differential equations, they propose:

$$[A]_t = \frac{\frac{k_1}{k_2} + [A]_0}{1 + \frac{k_1}{k_2[A]_0}\exp((k_1 + k_2[A]_0)t)} \tag{1}$$

In the original[1] and subsequent works,[2−8] the authors strongly contrast their nucleation and autocatalytic growth model against the earlier model proposed by LaMer, which proposes burst nucleation followed by 3-dimensional growth that is limited by diffusion[9] and with the phase-boundary controlled KJMA model of phase transformations.[10−14] Finke et al. rightly challenge the application of equilibrium concepts of classical nucleation theory to describe nanoparticle growth, and the ill-defined parameters of the KJMA model. (A correction to the KJMA model, by which all parameters are physically identified, the M-KJMA model, has subsequently been developed and evaluated both experimentally[15,16] and by simulation.[17] This corrected model yields the intrinsic rate constant, the velocity of the phase boundary, v_{pb}.) The F-W model, however, fails to address the impact of particle size, which is the fundamental basis for the sigmoidal kinetic effect they propose to be autocatalytic surface growth; i.e., the surface area of a sphere, for example, increases proportional to the square of its radius. Furthermore, as will be shown below, by treating nucleation and growth as parallel, rather than as serial processes, the k_1 and k_2 rate constants of the F-W model do not describe the unique processes.

Recently, Szabó and Lente reported a variant of the F-W model describing both nucleation and growth steps as second order reactions, $2C_1 \xrightarrow{k_n} C_2$ (nuc) followed by $C_i + C_1 \xrightarrow{k_g} C_{i+1}$ (growth), which result in a distinct set of differential equations.[18] Notably, they similarly consider the serial processes of nucleation and growth to be both continuous and parallel processes. In this present work detailed challenges to the F-W model are discussed, but the same issues arise with Szabó and Lente's consideration of k_n and k_g.

In defense of their F-W model,[1−8] they argue that the model was developed using an Occam's razor-based approach to mechanistic science which seeks the most minimal model to fully describe a system. Further they indicate their model was tested by "disproof", by which other models are considered and ruled out. Herein, they suggest, "The only even conceivable explanation [of the sigmoid kinetics] that we could come up with is summarized by the question: could a particle-size dependence alone give rise to the sigmoidal curves seen?" They go on to argue, "first and foremost, it is both physically and mathematically unreasonable that the analytic function... which was derived from autocatalysis as the growth pathway and which fits the sigmoidal curves quantitatively can simultaneously be the correct analytic function, and at all time values, for both autocatalysis and, separately but simultaneously, for the putative particle-size explanation."[1]

Notably, the impact of particle size was not directly tested with respect to their proposed model of nucleation and autocatalytic growth. And further, if particle size can account for the sigmoidal kinetic curves, then precisely the same logic could be used to rule out their proposed model.

A simple set of simulations of particle size and nucleation rate effects is described below, which clearly demonstrate that the k_1 and k_2 parameters derived from fitting to the F-W model, while appropriately fitting the sigmoidal shape of the kinetic curves, do not correspond to the actual rates of nucleation and growth.

This simplistic simulation cannot be directly tested against the LaMer equation, eq 2,[9] because no explicit solvent/particle

Received: July 17, 2019
Revised: August 13, 2019
Published: February 27, 2020

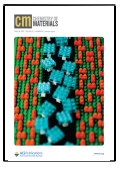

https://dx.doi.org/10.1021/acs.chemmater.9b02839
Chem. Mater. 2020, 32, 3651–3656

system with corresponding density, solubility, or diffusion characteristics is defined.

$$\frac{d}{dt}(x^2) = [C_{ss} - C_s(t)]\frac{2D}{\rho} - \frac{2D}{h^3}x^3 \quad (2)$$

where x is the radius of the particle, C_{ss} is the concentration of the super saturated solution, $C_s(t)$ is the concentration of the monomer above the saturation concentration at time t, D is the diffusion coefficient, ρ is the bulk density of the forming particle, and h is a limiting spherical solvent volume out of which the particle can grow.

However, this simple simulation can be tested against the M-KJMA model, eqs 3 and 4,[15−17] which explicitly considers particle size and reasonably reproduces the nucleation time and growth rate, thus providing a contrast to the F-W model.

$$\alpha(t) = 1 - \exp\{-[k_A(t - t_0)]^n\} \quad (3)$$

$$k_A = \frac{v_{pb}}{g\sqrt[3]{\frac{V}{i}}} \quad (4)$$

where $\alpha(t)$ is the fraction of the sample transformed at time t, k_A is the KJMA rate constant, t_0 is the time of initial nucleation, and the exponent n includes the dimensionality of the growth (1 to 3) plus the probability of nucleation (a value less clearly defined). Equation 4 modifies the classical KJMA rate expression[10−14] to yield the intrinsic growth rate constant, the velocity of the phase boundary, v_{pb}, where V is the volume of the sample, i is the number of initial nuclei, and g is a shape factor corresponding to the habit of particle growth.[15−17] For this simulation of spherical particle growth, $g = \left(\frac{3}{4\pi}\right)^{1/3}$. Note that the v_{pb} (units of distance/time) of the M-KJMA expression can be related to a mass/area·time rate by multiplying the v_{pb} by the density of the material.

Consider a sample of monomers, A, that grow into particles, B. The particle growth must start at some point in time, defined as its nucleation time, t_0. After the sample nucleates, let the simulated particle(s) grow at a rate described by the rate constant k_g, with units of distance (or amount of material) per time. In this simulation, simple spherical particle growth is assumed such that

$$B = 4/3\pi(k_g(t - t_0))^3 \quad (5)$$

where B is the volume of the particle or, if scaled by density, is the amount of material making up the particle. The total amount of material condensation may form many small particles or a single large particle, both scenarios being limited by the starting amount of A in the system. For this simple simulation, particles grow according to eq 5 until all material is consumed.

In a real system, termination effects must be considered at late stages of the reaction, caused either by a depletion in the concentration of A for materials growing out of solution or by impingement with other particles or the container walls for growth out of a condensed phase. Such termination effects are responsible for the sigmoidal shape at the end of the reaction.

To model termination effects, consider the simplest model of a sphere growing inside of a cubic volume. Initially the sphere will grow unimpinged (or in the fast diffusion limit with highest concentration of A). When the sphere meets the box edge, impingement sets in, at 52% transformation. The transformation is slowed as the final material is consumed. Such a simulated transformation is plotted in Figure 1, with two different growth rates, k_g = 0.02 distance/time (blue) and 0.04 distance/time (red).

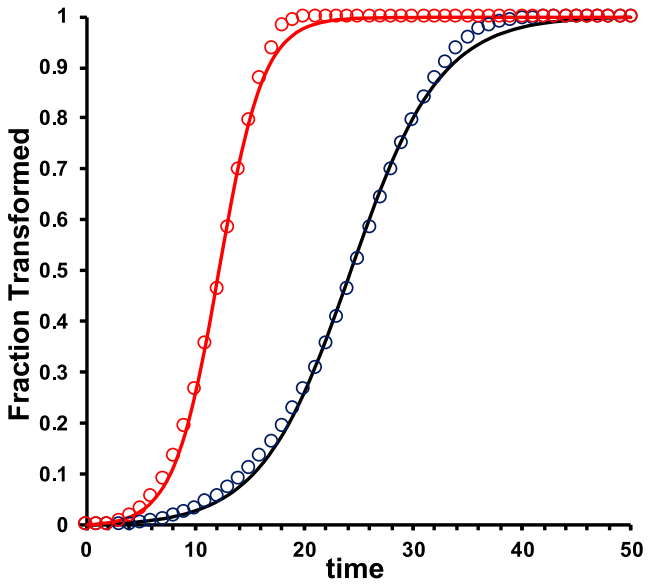

Figure 1. Normalized particle growth as a function of time of a single spherical particle growing into a cubic volume (eq 5, k_g = 0.02 (blue) and 0.04 (red) distance/time; t_0 = 0 time). Solid lines represent fits to the entire transformation using the F-W model.

Each simulation is then fit with the F-W model, eq 1, shown as the solid line curves in Figure 1, and by the M-KJMA model, eq 3 (Supporting Information Figure S1). The F-W and M-KJMA curves are essentially equivalent. The F-W parameters k_1 and k_2 and M-KJMA parameters k_A and n (t_0 = 0), for each scenario, are given in Table 1.

Table 1. F-W Rate Constants and M-KJMA Parameters with t_0 = 0 for Simulated Growth of a Single Spherical Particle within a Restricted Cubic Volume at Two Growth Rates, k_g (distance/time)

sim.	F-W		M-KJMA		
k_g	k_1	k_2	k_A	n	v_{pb}
0.02	6.80×10^{-4}	0.241	0.0374	3.98	0.023
0.04	1.34×10^{-3}	0.485	0.0749	4.00	0.046

It is important to note that for any individual particle there will be a single nucleating event which is followed by growth (secondary growth such as Ostwald ripening is ignored for this simple model). Given this, the significance of a nucleation rate constant, k_1, for an instantaneously nucleated single particle scenario is unclear. Furthermore, to fit this simulated data with the F-W model, both k_1 and k_2 rate constants double, whereas in the simulation only the explicitly defined growth rate constant k_g doubled. Thus, it is clear that k_1 and k_2 do not differentiate between nucleation and growth.

By contrast, the M-KJMA model fits the time dependent transformation data equally well (Supporting Information Figure S1). However, using eq 4 to correct the k_A to the v_{pb}, the M-KJMA model very nearly returns the simulation's explicitly defined k_g. The error between k_g and v_{pb} is notably

https://dx.doi.org/10.1021/acs.chemmater.9b02839
Chem. Mater. 2020, 32, 3651−3656

reduced if only the initial rate of the transformation is fit, a standard practice since termination effects are modeled poorly.

A slightly more complex simulation can be used to evaluate the effects of the formation of multiple nuclei and their formation at different rates, i.e., burst vs continuous nucleation. For these simulations, growth of each particle is allowed to proceed until all material is consumed, resulting in an abrupt termination, rather than trying to model more complex termination behavior that would result from nutrient depletion or sample impingement. Thus, the data is only fit to the first 50% of the transformation where termination effects should be minimal. Again the simulated transformation is fit with the F-W and M-KJMA models to evaluate the relevance of the parameters and thus the efficacy of the models.

The normalized transformation of the growth units into spherical particle(s) as a function of time according to eq 5, using a growth rate constant of k_g = 0.02 (distance/time), is shown in Figure 2 for four different nucleation scenarios. The

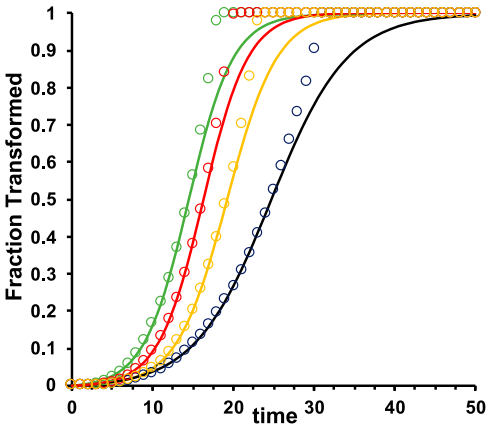

Figure 2. Spherical particle growth (eq 5, k_g = 0.02 distance/time) of one (blue) or five (green) particles nucleated in a burst or at continuous formation of five nuclei at rates of one nuclei/time step (red) and one nuclei/three time steps (yellow). Solid lines represent fits of the first 50% of growth using the F-W model.

blue curve represents the particle growth based on a single nucleation event while the green curve represents particle formation based on a burst of five nucleation events occurring at t = 0. The red and yellow curves represent continuous nucleation of five independent particles, the first nucleating at t = 0, but subsequent nuclei being formed at continuous rates of one nucleus per time step or one nucleus per every three time steps, respectively. Each scenario yields a sigmoidal growth curve but significantly different apparent rates of sample transformation. The presence of more nuclei, even with a constant particle growth rate, will result in a faster sample transformation.

The simulated particle growth scenarios, fit to 50% transformation, are each equally well described by the F-W model, shown as the solid line curves in Figure 2, and by the M-KJMA model (Supporting Information Figure S2). The F-W parameters k_1 and k_2 and M-KJMA parameters k_A and n (t_0 = 0), for each of these scenarios, is given in Table 2.

While the instantaneous single and burst of five nuclei simulations exhibit faster "nucleation" k_1 parameters than are observed for the simulations of continuous nucleation and the k_1 parameter is diminished between the 1 nucleus/(time step) and 1 nucleus/(3 time steps) rates, there is no apparent correlation between the rate constants and the actual nucleation rates defined in the simulation. Notably the k_2 growth rate constants do not resemble the common growth rate that was explicitly defined in the simulation for all scenarios. Instead k_2 is in some way responsive to the nucleation scenarios, i.e., larger for a greater number of particles, and thus is not a unique growth rate constant.

By contrast, when fit with the M-KJMA model, correcting the k_A rate constant for the single nucleus model by the geometric factor, $g = \left(\frac{3}{4\pi}\right)^{1/3}$, returns the v_{pb} = 0.022 distance/time, very close to the explicit simulation value of 0.02 distance/time. The M-KJMA fit to the scenario with a burst of 5 nuclei yields a k_A rate constant that is $(i/V)^{1/3} = (5)^{1/3}$ times larger than that for the single nucleus scenario. The M-KJMA model does not explicitly yield a nucleation rate; however, continuous nucleation, as opposed to burst nucleation, is reflected in an increased value of the exponent n. Furthermore, the ratio of k_A for the continuous nucleation scenarios to that of the single nucleation scenario yields the average value of i, summarized in Table 2, with which k_A can be corrected to v_{pb}.

An additional set of simulations test the efficacy of the F-W model to address reactions in which an induction time occurs before the onset of nucleation. We regularly observe such behavior in melt crystallization reactions (i.e., long periods at a supercooled state before nucleation and growth commences), and others have observed induction times in nanoparticle syntheses.[4,19]

Herein, a simulation is constructed whereby the above model of continuous nucleation of five nuclei at a rate of one nucleus per time step is modified by delaying the onset of nucleation by 5, 10, and 15 time steps. Again, particles are allowed to grow according to eq 5, with k_g = 0.02 distance/time, until all material is consumed; i.e., the simulation model does not include any impingement or depleted-concentration termination effects. The normalized transformation of the growth units into particles as a function of time under these conditions is shown in Figure 3. Rate parameters extracted by fitting the first 50% of the simulated data to the F-W (Figure

Table 2. F-W Rate Constants and M-KJMA Parameters with t_0 = 0, for Simulated Spherical Particle Growth with k_g = 0.02 Distance/Time and Variable Nucleation Scenarios

	F-W		M-KJMA			
	k_1	k_2	k_A	v_{pb}	n	i
single nucleus	1.14×10^{-3}	0.211	0.036	0.022	3.47	1
burst 5 nuclei	1.94×10^{-3}	0.360	0.062	0.022	3.48	5
1 nucleus/time step	1.01×10^{-3}	0.359	0.056	--	4.01	3.7
5 nuclei/3 time steps	6.67×10^{-4}	0.321	0.047	--	4.27	2.3

https://dx.doi.org/10.1021/acs.chemmater.9b02839
Chem. Mater. 2020, 32, 3651−3656

3) and M-KJMA models (Supporting Information Figure S3) are given in Table 3.

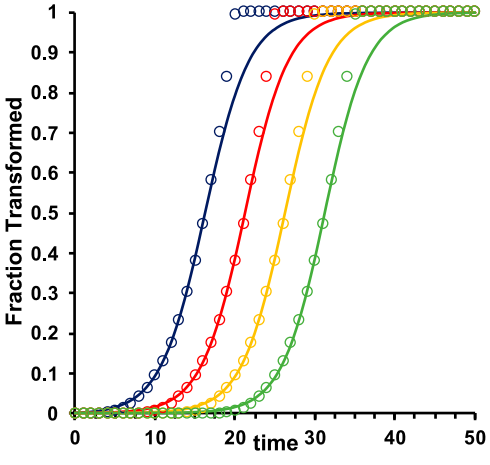

Figure 3. Spherical Particle Growth (eq 5, k_g = 0.02 distance/time) with continuous formation of five nuclei at a rate of one nuclei/time step with induction times of 0 (blue), 5 (red), 10 (yellow), and 15 (green) time steps. Solid lines represent fits of the first 50% of growth using the F-W model.

Table 3. F-W Rate Constants and M-KJMA Parameters with *n* Fixed to 4.01, for Simulated Spherical Particle Growth with k_g = 0.02 Distance/Time and Nucleation Rates of One Nucleus per Time Step for Five Nuclei, but with Induction Times of 0, 5, 10, and 15 Time Steps

	F-W		M-KJMA	
induction time	k_1	k_2	k_A	t_0
0	1.01×10^{-3}	0.360	0.055	−0.1
5	1.50×10^{-4}	0.366	0.055	4.9
10	2.35×10^{-5}	0.368	0.055	9.9
15	3.18×10^{-6}	0.374	0.055	14.9

The two-step F-W model has no provision for an actual induction time, instead suggesting that nucleation begins at the onset of the reaction. Later F-W models impute a four-step model that accounts for some induction time effects.[5] The induction time of this simulation, however, is sufficiently fit with the 2-step model such that the 4-step model would unlikely be utilized. More recently Bentea, Watzky, and Finke identified a $t_{induction}$ parameter, as well as t_{max} and t_2 parameters, to distinguish the lag, growth, and plateau phases of the reaction by evaluation of the first through third derivatives of the 2-step F-W model.[7]

Before considering the recently introduced F-W $t_{induction}$, t_{max}, and t_2 parameters,[7] it is important to note that the k_1 and k_2 parameters from fitting to the two-step F-W model, eq 1, show that delaying the onset of nucleation by some specific time, here 0 to 15 time steps, results in a k_1 nucleation rate constant that is slowed by almost 3 orders of magnitude even though the explicit rate of nucleation defined in the simulation is equivalent for all scenarios. The actual induction time has a minimal impact on the k_2 parameter, albeit a slight acceleration in the growth rate constant is implied for the simulations with increasing induction time.

When fitting the simulations with the M-KJMA model to extract the k_A and t_0 parameters, the parameter n was fixed to the value 4.01 obtained from the above zero-induction time scenario. Because the three parameters k_A, n, and t_0 are highly correlated in the KJMA model, it is unwise to ever fit more than two parameters; n can even be fixed to 3 based on an external observation of isotropic particle shape, and reasonable parameters will still be obtained.[17] Again, the sigmoidal curves produced by the M-KJMA model are equivalent to those produced by the F-W model, with only minor variation in the termination region. Notably, no variation in the k_A rate constant is observed for the variable induction time scenarios, and the fit t_0 value accurately represents the values explicitly defined in the simulation. Correcting the k_A value with the spherical growth factor, g, and the average i = 3.7 for this set of nucleation/growth conditions (see Table 2) returns ν_{pb} = 0.022 distance/time, effectively reproducing the rate explicitly defined in the simulation of 0.02 distance/time.

What then is the significance of the F-W $t_{induction}$, t_{max}, and t_2 parameters? Do these identified points correspond to physical features that can be identified from a simulation? To test this, the first through third derivatives, $d^n\alpha/dt^n$, where α is the fraction of the sample transformed, for the simulation of the spherical particle growing in a cubic box as described above for Figure 1 and Table 1, with t_0 = 0 time and k_g = 0.02 distance/time, are evaluated using a Savitzky−Golay method.[20] These are plotted in Figure 4.

The t_{max} is the maximum $d\alpha/dt$ and where $d^2\alpha/dt^2 = 0$, shown as the blue dashed line in Figure 4. Notably, this point is exactly equivalent to the point in the simulation where the growing spherical particle meets the edge of the confinement box. Beyond this point, growth is impinged by the edges of the box. (The analogue to this condensed-phase growth model for solution reactions would be a point at which the concentration of reactant A is depleted such that there is a greater concentration of B surface reactant sites than available reactant A.) Thus, t_{max} identifies the end of unrestricted particle growth.

By contrast, the F-W $t_{induction}$, identified as the maximum of $d^2\alpha/dt^2$ and the first point where $d^3\alpha/dt^3 = 0$ (red dashed line in Figure 4), corresponds to no physical feature of the simulated particle growth. This point is fully within the region of unrestricted growth and has no relationship to any actual induction time that may precede nucleation at t_0. Shifting the actual induction time, as was done for the simulations shown in Figure 3, simply shifts the F-W $t_{induction}$ by the amount of the actual induction time but still places the F-W $t_{induction}$ fully with the region of unimpeded particle growth.

The point identified as t_2 is the minimum for $d^2\alpha/dt^2$ and the second point where $d^3\alpha/dt^3 = 0$ (red dotted line in Figure 4). Like $t_{induction}$, t_2 corresponds to no physical feature of the particle growth. In this simulation, the t_2 point happens to be close to the onset of the secondary impingement of growth, where, in the final stages of the reaction, the nearly tetrahedral corners of the cube are the last vestiges of the sample that can grow (green dashed line in Figure 4).

Notably, while the F-W t_{max} parameter corresponds to the physical point of the onset of restricted growth but the F-W $t_{induction}$ and t_2 parameters correspond to no physical features, all three parameters are a reflection of the relative regions of unrestricted vs restricted growth. With otherwise equivalent nucleation and growth parameters, t_0 and k_g of eq 5, the F-W t_{max}, $t_{induction}$, and t_2 parameters[7] will change if the boundary conditions or location of nucleation within the box change. Thus, while the $t_{induction}$, t_{max}, and t_2 parameters may provide useful information about the overall reaction conditions, they provide no information directly pertaining to particle growth.

https://dx.doi.org/10.1021/acs.chemmater.9b02839
Chem. Mater. 2020, 32, 3651−3656

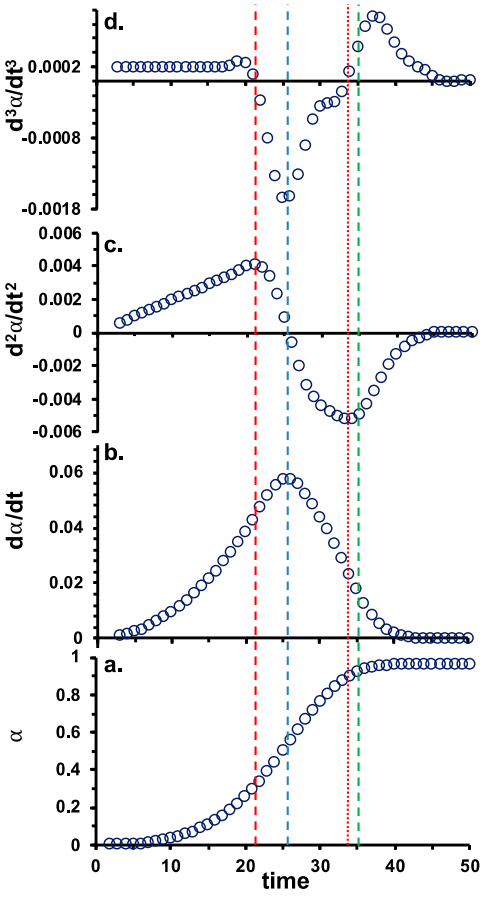

Figure 4. (a) Normalized particle growth, α, as a function of time of a single spherical particle growing into a cubic volume (eq 5, k_g = 0.02 distance/time; t_0 = 0). (b) $d\alpha/dt$, (c) $d^2\alpha/dt^2$, and (d) $d^3\alpha/dt^3$. The F-W $t_{induction}$ and t_2 parameters are represented by red dashed and dotted lines, respectively. The t_{max}, which is also the point of initial growth impingement, is represented by the blue dashed line, and the point of secondary impingement is represented by the green dashed line.

The simple simulations reported above demonstrate that the F-W model(s),[1−8] while accurately fitting sigmoidal kinetic growth curves, do not accurately describe nucleation or growth. By failing to account for the particle size, the number of nucleation events, and/or the possibility of an actual induction time, inaccurate physical conclusions likely will be drawn based on a F-W analysis.

The simulations here show the M-KJMA model to return the actual particle growth rate with reasonable accuracy and to identify the existence of any actual induction time. However, it is important to note that this set of simulations and analysis in no way seeks to imply that the M-KJMA model is the accurate model for nanoparticle growth. Most importantly, that model does not begin to address ligand or solvent termination effects. Nevertheless, the M-KJMA analysis demonstrates clearly that any model of actual particle growth must include particle size, nucleation frequency, and initial nucleation time parameters.

James D. Martin orcid.org/0000-0001-7414-2683

■ ASSOCIATED CONTENT

Supporting Information

The Supporting Information is available free of charge at https://pubs.acs.org/doi/10.1021/acs.chemmater.9b02839.

Three figures comparing the fit of the simulations to the F-W and M-KJMA models (PDF)

Table of simulated data (PDF)

■ AUTHOR INFORMATION

Complete contact information is available at: https://pubs.acs.org/10.1021/acs.chemmater.9b02839

Notes

The author declares no competing financial interest.

■ ACKNOWLEDGMENTS

This work was supported by NSF via Contract DMR-1709370

■ REFERENCES

(1) Watzky, M. A.; Finke, R. G. Transition Metal Nanocluster Formation Kinetic and Mechanistic Studies. A new Mechanism when Hydrogen Is the Reductant: Slow, Continuous Nucleation and Fast Autocatalytic Surface Growth. *J. Am. Chem. Soc.* **1997**, *119*, 10382−10400.

(2) Besson, C.; Finney, E. E.; Finke, R. G. A Mechanism for Transition-Metal Nanoparticle Self-Assembly. *J. Am. Chem. Soc.* **2005**, *127*, 8179−8184.

(3) Finney, E. E.; Finke, R. G. Nanocluster nucleation and growth kinetic and mechanistic studies: A review emphasizing transition-metal nanoclusters. *J. Colloid Interface Sci.* **2008**, *317*, 351−374.

(4) Watzky, M. A.; Finney, E. E.; Finke, R. G. Transition-Metal Nanocluster Size vs Formation Time and the Catalytically Effective Nucleus Number: A Mechanism-Based Treatment. *J. Am. Chem. Soc.* **2008**, *130*, 11959−11969.

(5) Finney, E. E.; Finke, R. G. Fitting and Interpreting Transition-Metal Nanocluster Formation and Other Sigmoidal Kinetic Data: A More Thorough Testing of Dispersive Kinetics vs Chemical-Mechanism-Based Equations and treatments for 4-Step Type Kinetic Data. *Chem. Mater.* **2009**, *21*, 4468−4479.

(6) Finney, E. E.; Finke, R. G. Is There a Minimal Chemical Mechanism Underlying Classical Avrami-Erofe'ev Treatments of Phase Transformation Kinetic Data. *Chem. Mater.* **2009**, *21*, 4692−4705.

(7) Bentea, L.; Watzky, M. A.; Finke, R. G. Sigmoidal Nucleation and Growth Curves Across Nature Fit by the Finke-Watzky Model of Slow Continuous Nucleation and Autocatalytic Growth: Explicit Formulas for the Lag and Growth Times Plus Other Key Insights. *J. Phys. Chem. C* **2017**, *121*, 5302−5312.

(8) Özkar, S.; Finke, R. G. Nanoparticle Formation Kinetics and Mechanistic Studies Important to Mechanism-Based Particle Size Control: Evidence for Ligand-Based Slowing of the Autocatalytic Surface Growth Step Plus Postulated Mechanisms. *J. Phys. Chem. C* **2019**, *123*, 14047−14057.

(9) LaMer, V. K.; Dinegar, R. H. Theory, Production and Mechanism of Formation of Monodispersed Hydrosols. *J. Am. Chem. Soc.* **1950**, *72*, 4847−4854.

(10) Kolmogorov, A. On the statistical theory of the crystallization of metals. *Bull. Acad. Sci. USSR* **1937**, *3*, 355−359.

(11) Johnson, W. A.; Mehl, R. F. Reaction Kinetics in Processes of Nucleation and Growth. *T. Am. I. Min. Met. Eng.* **1939**, *135*, 416−442.

(12) Avrami, M. Kinetics of Phase Change. I General Theory. *J. Chem. Phys.* **1939**, *7*, 1103−1112.

(13) Avrami, M. Kinetics of Phase Change. II Transformation-time relations for random distribution of nuclei. *J. Chem. Phys.* **1940**, *8*, 212−224.

(14) Avrami, M. Granulation, Phase Change, and Microstructure Kinetics of Phase Change. III. *J. Chem. Phys.* **1941**, *9*, 177−184.

(15) Dill, E. D.; Josey, A. A.; Folmer, J. C. W.; Hou, F.; Martin, J. D. Experimental determination of the crystallization phase boundary velocity in the halozeotype CZX-1. *Chem. Mater.* **2013**, *25*, 3932−3940.

(16) Hillis, B. G.; Losey, B. P.; Weng, J.; Ghaleb, N.; Hou, F.; Martin, J. D. From Rate Measurements to Mechanistic Data for Condensed Matter Reactions: A case study using the crystallization of $[Zn(OH_2)_6][ZnCl_4]$. *Crystals* **2017**, *7*, 11.
(17) Dill, E. D.; Folmer, J. C. W.; Martin, J. D. Simulating crystallization to elucidate the parameter space in the KJMA condensed phase transformation model. *Chem. Mater.* **2013**, *25*, 3941−3951.
(18) Szabó, R.; Lente, G. Full Analytical Solution of a Nucleation-Growth Type Kinetic Model of Nanoparticle Formation. *J. Math. Chem.* **2019**, *57*, 616−631.
(19) Chiu, G.; Meehan, E. J. Monodisperse Sulfur Sols from the Air Oxidation of Hydrogen Sulfide Solutions. *J. Colloid Interface Sci.* **1977**, *62*, 1−6.
(20) Savitzky, A.; Golay, M. J. E. Smoothing and Differentiation of Data by Simplified Least Squares Procedures. *Anal. Chem.* **1964**, *36*, 1627−1639.

https://dx.doi.org/10.1021/acs.chemmater.9b02839
Chem. Mater. 2020, 32, 3651−3656